Thiol-yne chemistry for 3D printing: Exploiting an off-stoichiometric route for selective functionalization of 3D objects

Thiol-yne chemistry for 3D printing: exploiting off stoichiometric route for selective functionalization of 3D objects

Ignazio Roppolo,[a] Francesca Frascella[a], Matteo Gastaldi[b], Betty Ciubini[a], Claudia Barolo [b], Luciano Scaltrito[a], Carmelo Nicosia [c] Marco Zanetti[b,d] and Annalisa Chiappone*[a]

Department of Applied Science and Technology DISAT, Politecnico di Torino, Corso Duca degli Abruzzi, 24, Torino, 10129, Italy

Department of Chemistry and NIS Centre, University of Turin, Via P. Giuria 7, Torino, 10125, Italy

Department of Electronics and Telecommunications DET, Politecnico di Torino, Corso Duca degli Abruzzi, 24, Torino, 10129, Italy

ICxT Centre, University of Turin, Lungo Dora Siena 100, Torino, 10153, Italy

An alkyne monomer based on bis(propargyl) fumarate is sinthetized and used to produce DLP-3D printable formulations with a thiols exploiting photoinduced thiol-yne reaction. By preparing mixtures containing different relative ratios of the two monomers, it is possible to obtain polymers exposing different unreacted functional groups on their surface. The reactivity of the formulations toward visible light irradiation is studied by ATR analyses and photorheology tests, the printability with a DLP equipment is demonstrated and the thermomechanical properties of the obtained polymers are investigated by DMA. Changing the printing formulation during the printing process, objects exposing either triple bonds or thiol groups or a mix of it can be obtained; this property can be exploited to selectively functionalize the built parts in a dedicated post process. As a proof of concept, a simple hybrid structure is treated with a squaraine dye azide terminated, to exploit a 'click' reaction with the alkyne groups available. The fluorescence of the functionalized structure is observed with a spinning disk confocal microscope. Such strategy can allow to produce 3D objects with controllable structure just by varying the relative ratio of the co- monomers in the formulations during the printing process.

Introduction

3D printing is a production technique that allows to fabricate objects starting from CAD files by adding material in a layer by layer fashion.[1] The techniques comprised under this umbrella term enable the fabrication of extremely complex shapes without material waste and without using moulds.[2, 3] This makes 3D printing a step forward and fascinating alternative to the most common subtractive manufacturing procedures. [4-6]

In the last decades several types of 3D printing machines have been developed and optimized; they differ from each other for the technology that they exploit and for the typology of printable materials.[1] Just considering the polymeric materials, many different classes of 3D printers can be listed, some examples are: FFF (Fused Filament Fabrication), the most diffused technique that uses thermoplastic filaments, heated and deposited layer by layer;[7] SLS (Selective Laser Sintering), that sinters thermoplastic powders with a laser to obtain 3D objects;[8] SL (Stereo Lithography) and its close relative DLP (Digital Light Processing), that print thermoset polymers starting from liquid photocurable formulations. Those mixtures are usually based on (meth)acrylic monomers. [9, 10] Each technique has its advantages and drawbacks and the choice of a particular one can be related to the specific application.[11] Nowadays, all the 3D printing techniques are largely investigated at the academic level and in some cases the additive manufacturing products are proposed at the commercial level.[1, 12]

To further expand the possibilities given by 3D printing, functional 3D shaped objects can be fabricated.[13, 14] In this work, we developed new functional materials for photopolymerization based processes, in particular DLP. [15]

Intrinsically, functional 3D printable materials for DLP or SL have been previously proposed;[15] in this case, several routes can be followed such as the addition of nanofillers,[13, 16, 17 18] the use of stimuli responsive,[19] conductive[20] or shape memory polymers,[21] smart dyes[22] and may others.[23 15]

Another suitable approach consists in exploiting a post functionalization step on the 3D printed objects; this can result particularly interesting for the introduction of biofunctional molecules, as largely demonstrated for different polymeric surfaces.[24] To do this, chemically reactive moieties can be directly introduced in the DLP printable liquid formulations, aiming to exploit their available groups for further functionalization steps.

Stassi et al.[25] printed micrometric cantilevers by DLP starting from an acrylate-based formulation in which acrylic acid was added. Its carboxylic groups were exploited to functionalize the cantilever surface. Alternatively, Wang et al.[26] incorporated a vinyl-terminated initiator into the curable resin to obtain functional structural materials that enabled a post-printing surface-initiated ATRP modification.

The addition of chemical moieties that can easily react in a dedicated functionalization step could enable a wide range of reactions for the modification of 3D printed objects.[27, 28] In this work, we propose the use of 3D printable thiol-yne monomers to obtain objects that can be easily post functionalized.[29, 30]

Thiol-yne polymerization has been studied since many decades,[31-34] but in the last years it attracted an increasing interest in the field of photopolymerization [35]since, as well as thiol-ene reactions,[36] it presents many advantages over the more common, traditional radical chain-growth polymerizations. [37]

Alkynes monomers can be easily synthesized in different structural formats. In the thiol-yne reaction each alkyne functional group can react consecutively with two thiol functional groups; this leads to the formation of highly crosslinked networks presenting high toughness and good thermo-mechanical properties, beyond their known biocompatibility.[38] These intriguing properties make thiol-yne photopolymerization an interesting route for the production of films with good mechanical properties. [35] But, making a step ahead, this kind of chemistry can also be applied to DLP and SL 3D printing, allowing the production of 3D materials presenting the afore mentioned characteristics.[39]

To allow an easy post-functionalization of these 3D printable materials, we propose the development of off-stoichiometry formulations: in this way, after the printing process, the excess of SH (thiol) or YNE (alkyne) functionalities not involved in the cross-linked network, results available for a variety of post-functionalization processes. As Carlborg et al.[40] introduced the idea of using OSTE (off-stoichiometry thiol-ene) formulations manly for developing functionalized microfluidic channels;[41] in this paper we prepare OSTY (off-stoichiometry thiol-yne) formulations. After the synthesis of the alkyne monomer (bis(propargyl) fumarate), we demonstrate its printability and the possibility to post functionalize the 3D printed parts. Such strategy can allow to produce 3D objects with controllable networks, just by varying the relative ratio of the co- monomers in the formulations during the printing process.

Experimental

Materials

All chemicals were purchased from Sigma-Aldrich, Fluka, Merck Riedel de Haen and Alfa Aesar, unless otherwise noted and were used as received. The synthesis of the squaraine was carried out with the microwave BIOTAGE® Isolera Iniziator + 2.5. All flash purifications were performed with BIOTAGE® Isolera™ using Biotage® SNAP Ultra silica gel column. TLC were performed on silica gel 60 F254 plates.

Trimethylolpropane tris(3-mercaptopropionate) (Sigma-Aldrich) was used as thiol comonomer, Phenylbis(2,4,6-trimethylbenzoyl) phosphine oxide (BAPO, Sigma-Aldrich) was used as photoinitiator.

Synthesis of bis(propargyl) fumarate – alkyne monomer

The reaction, requiring anhydrous conditions, was conducted in flame-dried glassware under an atmosphere of argon. As reported in Figure 1, propargyl alcohol (II) (7.55 mL, 131 mmol) was dissolved in anhydrous dichloromethane (50 mL) in a three-necked round-bottomed flask equipped with a stir bar and a dropping funnel. Triethylamine (21.88 ml, 157.2 mmol) was added, and the mixture cooled to 0 °C. A solution of fumaryl chloride (I) (5.65 mL, 52.4 mmol) in anhydrous CH_2Cl_2 (30 mL) was added dropwise over 45 minutes. The reaction mixture was allowed to reach room temperature and stirred for 24 hours and then washed sequentially with saturated ammonium chloride (3x 250 mL), saturated sodium bicarbonate (2 x 240 mL) and brine (1 x 80 mL) before being dried, filtered and the solvent evaporated. This provided crude material as a dark brown solid that was purified by flash column chromatography (isocratic elution with 100% diethyl ether) to obtain the product in 81 percent yield as a browned white solid. [42] Rf 0.87 (100% diethyl ether); ^{1}H NMR (600 MHz, Chloroform-d): δ 6.93 (s, 2H), 4.80 (d, J = 2.5 Hz, 4H), 2.52 (t, J = 2.5 Hz, 2H), ^{13}C NMR (151 MHz, Chloroform-d): δ 163.99, 133.69, 75.89, 75.39, 52.64.

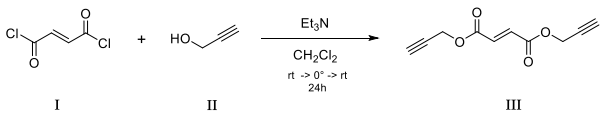

Figure 1 - Synthesis of bis(propargyl) fumarate. Experimental conditions: R: Et_3N, S: CH_2Cl_2, 45 min, 0°C; 0°C → rt; 24 h, rt.

Synthesis of 4-((1-(10-azidodecyl)-5-carboxy-3,3-dimethyl-3H-indol-1-ium-2-yl)methylene)-2-(((E)-1-butyl-5-carboxy-3,3-dimethylindolin-2-ylidene)methyl)-3-oxocyclobut-1-en-1-olate – squaraine dye azide terminated

Figure 2 – General procedure for the synthesis of the squaraine. (1) Anhydrous CH_3CN, MW: T=155°C, t=20 min. (2) EtOH, MW: T=90°C, t=13 min. (3) BuOH/Toluene, MW: T=160°C, t=60 min. (4) DMF, MW: T=100°C, t=20 min.

STEP 1: (1): The procedure followed is the same reported by N. Barbero et al.[43]

STEP 2: 1-butyl-5-carboxy-2,3,3-trimethyl-3H-indol-1-ium (0.100 g, 0.258 mmol) was put in a microwave vial, equipped with a magnetic stirring. Then ethanol (3 ml), 3,4-diethoxycyclobut-3-ene-1,2-dione (0.088 g, 0.08 ml, 0.52 mmol) and triethylamine (0.078 g, 0.11 ml, 0.78 mmol) were added. The reaction was carried out with the microwave (T=90°C, 13 minutes). The crude material was evaporated, was recovered with ethyl ether and was filtrated under vacuum: the obtained solid was washed with ethyl ether (3x15 ml). The product was in the filtrate that was evaporated and the liquid was diluted with dichloromethane and it was purified

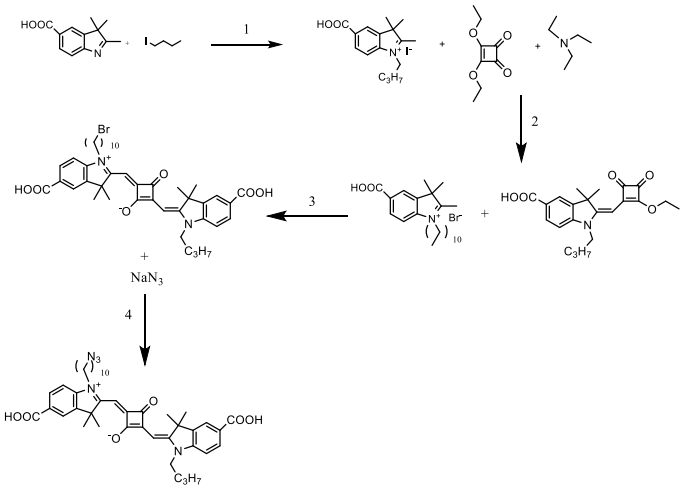

by flash column chromatography (EtOAc : Petroleum ether 3:7).

Yield: 49%

Rf: 0.28 (EtOAc : Petroleum ether 3:7)

STEP 3: 1-(10-bromodecyl)-5-carboxy-2,3,3-trimethyl-3H-indol-1-ium (0.145 g, 0.289 mmol) and 1-butyl-2-((2-ethoxy-3,4-dioxocyclobut-1-en-1-yl)methylene)-3,3-dimethylindoline-5-carboxylic acid (0.111 g, 0.289 mmol) were put in a vial and dissolved in butanol (1 ml) and toluene (1 ml). The vial was sealed and the reaction was carried out with the microwave (T=160°C, 1 hour). The green-blue liquid was recovered with ethyl ether and the solvent was evaporated. The product was re-crystallised by butanol and the obtained solid was filtered under vacuum, washed with ethyl ether and dried in the vacuum stove (40°C, 2 hours).

Yield: 24% (0.052 g, 0.069 mmol)

Rf: 0.71 (MeOH : $CHCl_3$ 1:9)

STEP 4: 4-((1-(10-bromodecyl)-5-carboxy-3,3-dimethyl-3H-indol-1-ium-2-yl)methylene)-2-(((E)-1-butyl-5-carboxy-3,3-dimethylindolin-2-ylidene)methyl)-3-oxocyclobut-1-en-1-olate (0.025 g, 0.033 mmol) and sodium azide (0.0024 g, 0.036 mmol) were added in a vial and dissolved in DMF (1 ml). The vial was sealed and the reaction was carried out with the microwave (T=100°C, 20 minutes). The product was transferred in

a separation funnel with CH_2Cl_2 and it was washed with brine and twice with deionized water. Then the product was dried with sodium sulphate, filtered and the solvent was evaporated under vacuum.

Preparation of the printable formulations Three different formulations were prepared by mixing the synthesized alkyne with the trifunctional thiol chosen. Different ratios of the two components were mixed in order to obtain a stoichiometric formulation (named EQ), one formulation with an excess of triple (named YNE) bonds and one last with an excess of SH groups (named TH, See SI for the concentration). In all the formulations 1 phr of BAPO was added and solubilized with the addition of few drops of acetone.

Printing process The 3DLPrinter-HD 2.0 (Robot Factory) equipped with a projector with a resolution of 50 µm in x and y (1920 × 480 × 1080 pixels) was used as printing apparatus. The Z resolution can be varied from 10 to 100 µm. The power density of the light source is 10 mW/cm^2. The irradiation time was settled for each formulation according to their reactivity (See SI). After printing, a post-curing process (3 min) was performed in air with a broad-band medium pressure mercury lamp, also provided by Robot Factory (UV power density 50 mW/cm^2).

Post functionalization process - Alkyne fluorescent labelling

A squaraine dye azide terminated was synthesized, able to perform a 'click' chemistry with the alkyne groups available on the 3D printed structure. The idea is to have a sensitive and robust methods for observing alkyne free groups exposed in the three different formulations (YNE, EQ and SH) after the 3D printing process. The post functionalization process reaction was performed following the procedure developed by A.B. Hughes et al. based on Cu-catalyzed in combination with terminal-alkynes.[44] In brief, the sample was added in a solution of 1 mmol squaraine dye azide terminated and Cu(0) powder in a 1:2 mixture of tBuOH:H_2O. After 2 hours, the 3D printed object was deeply washed in ethanol (3x 5ml) and dried in a nitrogen stream.

Characterization

Photorheology tests were performed with an Anton Paar rheometer (Physica MCR 302) in parallel plate. The instrument is coupled with a Hamamatsu LC8 lamp emitting in the visible range with a cut-off filter below 400 nm (intensity 10 mW/cm^2). The gap between the two plates was set to 0.3 mm and the sample was kept at 25°C, under constant shear frequency of 10 rad s^{-1}, light was turned on after 1 min in order to stabilize the system. The measurement was performed in the linear viscoelastic region (strain amplitude 5%)**.** The value of G' as a function of the irradiation time was collected for all the prepared samples.

ATR spectra were collected with a Nicolet iS50 FT-IR spectrometer (Thermo Scientific) equipped with an attenuated total reflection (ATR) accessory (Smart iTX). The spectra were collected firstly on a drop of the liquid photocurable formulations and then on the 3D printed samples after UV post curing. The conversion of the thiol group, triple and double bonds were evaluated calculating the decrease of the areas of the peaks at 2570 cm^{-1}, 2130 cm^{-1} and 1640 cm^{-1} respectively. The area of the peak was normalized by a constant signal in the spectra corresponding to the stretch of carbonyl group centred at 1750 cm^{-1}.

The thermal behaviour of the monomer was evaluated by DSC analysis using a METTLER DSC-30 (Greifensee, Switzerland) instrument with a ramp from RT to 150°C (10°C/min).

The thermomechanical properties of the printed materials were evaluated by DMA. 3D printed films were prepared (thickness, 300 µm) and tested using a Triton Technology TTDMA. The response of the samples was observed in the temperature range of −40 to 70 °C with a heating rate of 3 °C/min, at a frequency of 1 Hz and strain of 20 µm.

Bright-field and fluorescent images were collected using a microscope (model Eclipse Ti2 Nikon) coupled with a Crest X-Light spinning disk confocal and a Lumencor SPECTRA X light engine. All images displayed the same

scaling and were collected using a Plan Fluor 10x 0.3 NA and a Plan Apo 20x 0.75 NA(Nikon). A scan of large image at high magnification has been performed in order to have a whole overview of the sample.

Nuclear magnetic resonance 1H NMR (600 MHz) and 13C NMR (151 MHz) experiments were conducted using a Jeol ECZ-R 600 MHz instrument with deuterated chloroform (Sigma-Aldrich, 99.8 atom%) and deuterated DMSO. Chemical shifts were referenced to the solvent proton resonance (7.26 ppm for 1H NMR, 77.17 ppm for 13C NMR).

Results and discussion

After the synthesis, the alkyne monomer chosen (bis(propargyl) fumarate) was mixed with a trifunctional thiol, in different ratios, in order to obtain formulations with stoichiometric and off-stoichiometric (OSTY) compositions. Before printing, the reactivity of the liquid mixtures was assessed by photorheology tests (see SI). Following the variation of the elastic modulus upon visible light irradiation, it has been possible to observe that the stoichiometric formulation (EQ) and the one with the excess of thiols (TH) presented a good reactivity, similar to that of other formulations already proposed;[45] while the formulation with the excess of triple bonds (YNE) needed longer irradiation times. These observations allowed to set the printing parameters (see table S1 in SI).

Firstly, flat specimens (5x 20x 0.3 mm) were produced for each single formulation and then by changing the formulation during the printing process; this allowed to have samples presenting different excess of reactive groups on the different sides. Those specimens were used both for ATR and DMA measurements.

The conversion of the reactive groups was evaluated by ATR analysis comparing the spectra of the liquid formulations with those collected on the printed samples. The values of conversion are reported in Table 1 (Spectra reported in the SI file).

Table 1 Conversion of the reactive groups present in the formulation.

Sample	**-SH conversion (%)**	**-C≡C- conversion (%)**	**-C=C - conversion (%)**
EQ	**60**	**50**	**72**
YNE	**80**	**37**	**63**
TH	**48**	**98**	**100**

The values reported showed that the EQ specimen do not reach full conversion, and it presents both unreacted thiol and triple bond. This could be expected, considering that once the two monomers react the mobility of the system considerably decrease, preventing further reactions. As a matter of fact, this formulation results 3D printable, however the presence of both the species in a considerable amount makes this material not exploitable for selective functionalization. Differently, both the OSTY formulations present a more controllable behaviour. As expected, the TH formulation presents a complete reaction of unsaturated bonds, since they could react with the thiols present in their proximity. Similarly, the YNE formulation presents a very high conversion of –SH groups and a high number of remaining triple bonds. The alkyne still available has been exploited in the following functionalization step with the synthesized squaraine dye azide terminated.

The different matrices showed even a different thermal-mechanical behaviour, evaluated my means of Dynamic Mechanical Analysis, DMA (see Figure 3). DMA measurements showed that the 3D printed materials presented a higher glass transition temperature (T_g) by increasing the amount of yne monomer in the formulation, moving from 8 ˚C in the TH sample to 34 ˚C in YNE one.

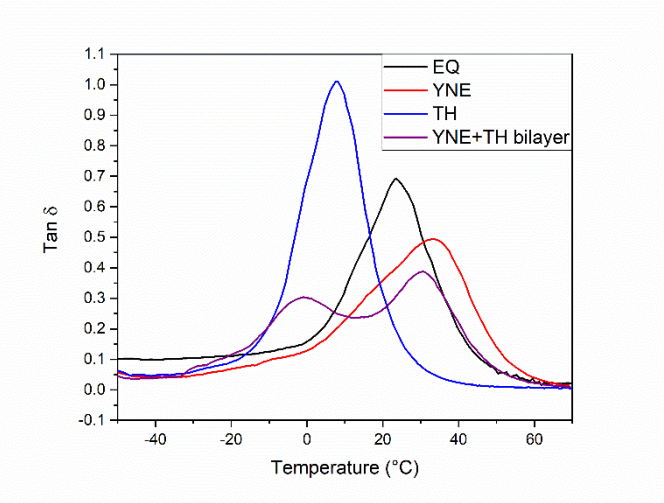

Figure 3 Tan δ plot obtained by DMA analyses on flat specimens produced with the three formulations (Off-stoichiometry TH, Off-stoichiometry YNE and stoichiometric EQ) and on one bilayer specimen built with the two OSTY formulation one after the other (TH and YNE).

This could be explained taking into account that the yne monomer gives rigidity to the system (see DSC of the monomer in SI file). This effect could be used to tune the desired properties of the final object. Moreover, a bilayer specimen was produced, changing the printable formulation at half of the printing process. As expected, the sample presented the two T_gs of the two off-stoichiometry materials, indicating that it is possible to print consecutively the two formulations maintaining the distinct properties.

The studied formulations allowed to print parts of different shapes with a good resolution, see figure 4. Furthermore, just by changing the formulation during the printing process, it has been possible to obtain objects exposing different functional groups (-SH or alkyne) along their z axis (Figure 4). A good adhesion of the different layers was also observed after printing and post curing.

By choosing a dye, which selectively reacts towards the alkyne groups still available in the 3D printed object, we demonstrated that the printed structures can be easily and specifically functionalized. As expected from the ATR analysis and conversion of the reactive groups, the triple bonds were available in different amounts in the three formulations, accordingly to their (TH, EQ and YNE).

In Figure 4A, the results of the post functionalization step with the squaraine dye azide terminated, for the 3D printed object obtained starting from the three selected printable formulation, two off stoichiometry (YNE and TH) and the stoichiometric one (EQ).

As stated, it was evident a trend in the color change, from native white to blue (due to squaraine dye presence), of the three different specimens. In particular, there was no evidence of dye functionalization in the off-stoichiometry TH sample, while there was an increasing dye linkage in the EQ and OSTY YNE, respectively.

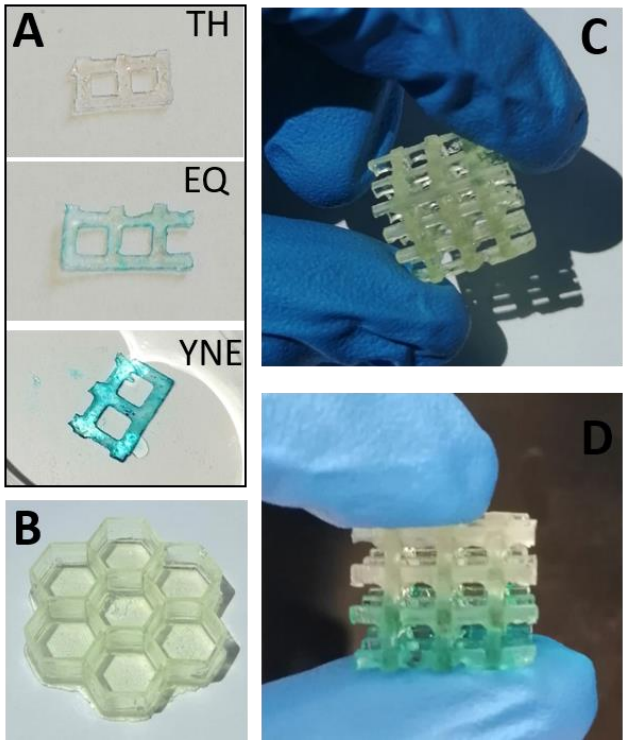

Figure 4 Images of the 3D printed objects. A) result of the post functionalization step with the squaraine dye for the three formulations (Off-stoichiometry TH, Off-stoichiometry YNE and stoichiometric EQ). B) Structure built with the stoichiometric formulation (EQ) C) Hybrid structure with the two off stoichiometric formulations (YNE at the bottom and TH on top) D) result of the post functionalization process on the same structure.

To further demonstrate the selectivity of the post functionalization, due to the squaraine dye azide terminated reacting with the OSTY YNE; a fluorescent imaging study was performed on a slice obtained from the hybrid structure (Figure 4 D). The sample was selected along the z axis (hybrid structure with the two OSTY formulations), so to be representative of the whole 3D printed object. When the fluorescence dye (squarine azide terminated) was grafted on the specimen, it was possible to produce a fluorescence image of the different printed layers.

To provide a wider field-of-view, a scan of large image was performed (72 scans with a 10x objective), as shown in Figure 5. The wide field fluorescent image (Figure 5 B) clearly state the different triple bond conversion, between the two OSTY formulations. The blue fluorescence signal due to squaraine dye functionalization was really intense in the YNE part (top of the image) and only barely visible in the TH area (bottom of the image). As a result, the fluorescent study exhibits a sharp edge in the interface area, verifying the possibility to a selective functionalization of the 3D printed object, only by changing along the z-axis its stoichiometry.

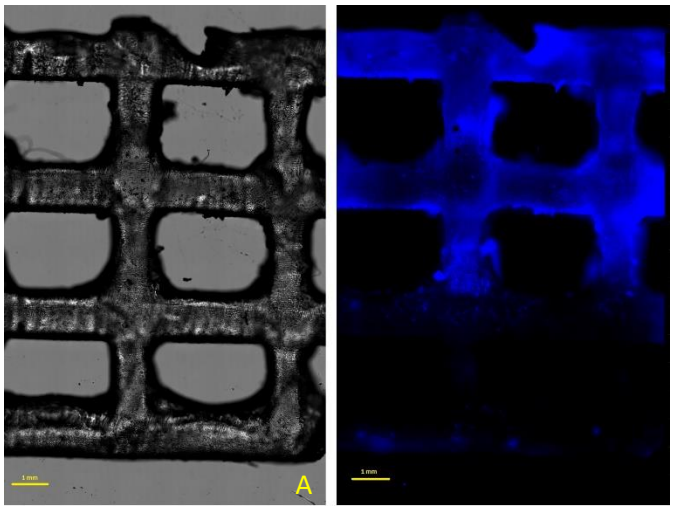

Figure 5 Wide field optical detection (A - bright field, B – fluorescence) of the slice obtained from the 3D printed hybrid structure (scale bar 1 mm). The sample was functionalized with a solution 1 mmol of squaraine azide terminated.

Conclusions

In this work, we demonstrated that thiol-yne chemistry is an available strategy for the production of new 3D printable materials. Moreover, the development of off stoichiometry thiol-yne formulations (OSTY) allows the possibility to locally tune the characteristics of the network, exposing selectively desired moieties (either alkyne or thiol groups) that could be exploited for a further functionalization step. We reached this goal by successful grafting of squarine dyes with azide moieties.

The strategy here proposed opens new perspective for the fabrication of functional 3D printed structures, in particular for biomedical field in which multiple functionalization could be a key-point to the development of next generation devices.

Conflicts of interest

There are no conflicts to declare.

Acknowledgements

The present work was performed in the framework and financed by POLITO BIOMed LAB, an interdepartmental laboratory financed by Politecnico di Torino. DEFLeCT (“Advanced platform for the early detection of not small cells lung cancer”, Piedmont “Health &WellBeing” Platform) project. funded by Regione Piemonte POR-FESR 2014-2020. HYDROLIGHT (“Reversible 3D light-structuring of stimuli-responsive hydrogel networks for biophotonic applications”), funded by Politecnico di Torino 2017-2019.

Notes and references

1. T. D. Ngo, A. Kashani, G. Imbalzano, K. T. Q. Nguyen and D. Hui, *Composites Part B: Engineering*, 2018, **143**, 172-196.

2. B. C. Gross, J. L. Erkal, S. Y. Lockwood, C. Chen and D. M. Spence, *Analytical Chemistry*, 2014, **86**, 3240-3253.

3. R. L. Truby and J. A. Lewis, *Nature*, 2016, **540**, 371.

4. S. C. Ligon, R. Liska, J. Stampfl, M. Gurr and R. Mülhaupt, *Chemical Reviews*, 2017, **117**, 10212-10290.

5. M. Hofmann, *ACS Macro Letters*, 2014, **3**, 382-386.

6. N. Bhattacharjee, A. Urrios, S. Kang and A. Folch, *Lab on a Chip*, 2016, **16**, 1720-1742.

7. E. Cuan-Urquizo, E. Barocio, V. Tejada-Ortigoza, B. R. Pipes, A. C. Rodriguez and A. Roman-Flores, *Materials*, 2019, **12**.

8. F. Shen, S. Yuan, C. K. Chua and K. Zhou, *Journal of Materials Processing Technology*, 2018, **254**, 52-59.

9. A. Bagheri and J. Jin, *ACS Applied Polymer Materials*, 2019, **1**, 593-611.

10. J. Zhang and P. Xiao, *Polymer Chemistry*, 2018, **9**, 1530-1540.

11. A. Bandyopadhyay and S. Bose, *Additive Manufacturing*, CRC Press, 2015.

12. J.-Y. Lee, J. An and C. K. Chua, *Applied Materials Today*, 2017, **7**, 120-133.

13. M. Nadgorny and A. Ameli, *ACS Applied Materials & Interfaces*, 2018, **10**, 17489-17507.

14. Z. X. Khoo, J. E. M. Teoh, Y. Liu, C. K. Chua, S. Yang, J. An, K. F. Leong and W. Y. Yeong, *Virtual and Physical Prototyping*, 2015, **10**, 103-122.

15. M. Layani, X. Wang and S. Magdassi, *Advanced Materials*, 2018, **30**, 1706344.

16. G. Gonzalez, A. Chiappone, I. Roppolo, E. Fantino, V. Bertana, F. Perrucci, L. Scaltrito, F. Pirri and M. Sangermano, *Polymer*, 2017, **109**, 246-253.

17. V. C.-F. Li, X. Kuang, A. Mulyadi, C. M. Hamel, Y. Deng and H. J. Qi, *Cellulose*, 2019, **26**, 3973-3985.

18. J. Bustillos, D. Montero-Zambrano, A. Loganathan, B. Boesl and A. Agarwal, *Polymer Composites*, 2019, **40**, 379-388.

19. R. T. Shafranek, S. C. Millik, P. T. Smith, C.-U. Lee, A. J. Boydston and A. Nelson, *Progress in Polymer Science*, 2019, **93**, 36-67.

20. G. Scordo, V. Bertana, L. Scaltrito, S. Ferrero, M. Cocuzza, S. L. Marasso, S. Romano, R. Sesana, F. Catania and C. F. Pirri, *Materials Today Communications*, 2019, **19**, 12-17.

21. M. Zarek, M. Layani, I. Cooperstein, E. Sachyani, D. Cohn and S. Magdassi, *Advanced Materials*, 2016, **28**, 4449-4454.

22. F. Frascella, G. González, P. Bosch, A. Angelini, A. Chiappone, M. Sangermano, C. F. Pirri and I. Roppolo, *ACS Applied Materials & Interfaces*, 2018, **10**, 39319-39326.

23. H. H. Hwang, W. Zhu, G. Victorine, N. Lawrence and S. Chen, *Small Methods*, 2018, **2**, 1700277.

24. F. Abbasi, H. Mirzadeh and A.-A. Katbab, *Polymer International*, 2001, **50**, 1279-1287.

25. S. Stassi, E. Fantino, R. Calmo, A. Chiappone, M. Gillono, D. Scaiola, C. F. Pirri, C. Ricciardi, A. Chiadò and I. Roppolo, *ACS Applied Materials & Interfaces*, 2017, **9**, 19193-19201.

26. X. Wang, X. Cai, Q. Guo, T. Zhang, B. Kobe and J. Yang, *Chemical Communications*, 2013, **49**, 10064-10066.

27. J. M. Goddard and J. H. Hotchkiss, *Progress in Polymer Science*, 2007, **32**, 698-725.

28. R. M. Arnold, N. E. Huddleston and J. Locklin, *Journal of Materials Chemistry*, 2012, **22**, 19357-19365.

29. R. M. Hensarling, V. A. Doughty, J. W. Chan and D. L. Patton, *Journal of the American Chemical Society*, 2009, **131**, 14673-14675.

30. H. Nandivada, X. Jiang and J. Lahann, *Advanced Materials*, 2007, **19**, 2197-2208.

31. A. B. Lowe, C. E. Hoyle and C. N. Bowman, *Journal of Materials Chemistry*, 2010, **20**, 4745-4750.

32. K. Griesbaum, *Angewandte Chemie International Edition in English*, 1970, **9**, 273-287.

33. A. B. Lowe, *Polymer*, 2014, **55**, 5517-5549.

34. A. Massi and D. Nanni, *Organic & Biomolecular Chemistry*, 2012, **10**, 3791-3807.

35. J. W. Chan, J. Shin, C. E. Hoyle, C. N. Bowman and A. B. Lowe, *Macromolecules*, 2010, **43**, 4937-4942.

36. C. E. Hoyle and C. N. Bowman, *Angewandte Chemie International Edition*, 2010, **49**, 1540-1573.

37. B. D. Fairbanks, T. F. Scott, C. J. Kloxin, K. S. Anseth and C. N. Bowman, *Macromolecules*, 2009, **42**, 211-217.

38. A. Oesterreicher, C. Gorsche, S. Ayalur-Karunakaran, A. Moser, M. Edler, G. Pinter, S. Schlögl, R. Liska and T. Griesser, *Macromolecular Rapid Communications*, 2016, **37**, 1701-1706.

39. A. Oesterreicher, J. Wiener, M. Roth, A. Moser, R. Gmeiner, M. Edler, G. Pinter and T. Griesser, *Polymer Chemistry*, 2016, **7**, 5169-5180.

40. C. F. Carlborg, T. Haraldsson, K. Öberg, M. Malkoch and W. van der Wijngaart, *Lab on a Chip*, 2011, **11**, 3136-3147.

41. F. Saharil, C. F. Carlborg, T. Haraldsson and W. van der Wijngaart, *Lab on a Chip*, 2012, **12**, 3032-3035.

42. E. R. Gillies, B. Fan, A. D. WongJohn, F. Trant. US10214609B2, 2019.

43. N. Barbero, C. Magistris, J. Park, D. Saccone, P. Quagliotto, R. Buscaino, C. Medana, C. Barolo and G. Viscardi, *Organic Letters*, 2015, **17**, 3306-3309.

44. O. D. Montagnat, G. Lessene and A. B. Hughes, *Tetrahedron Letters*, 2006, **47**, 6971-6974.

45. A. Chiappone, I. Roppolo, E. Naretto, E. Fantino, F. Calignano, M. Sangermano and F. Pirri, *Composites Part B: Engineering*, 2017, **124**, 9-15.

Ref 42 E. R. Gillies, B. Fan, A. D. WongJohn, F. Trant. US10214609B2, 2019.